

Enhanced resonance frequency in Co_2FeAl thin film with different thicknesses grown on flexible graphene substrate

Cai Zhou(周偲), Shaokang Yuan(袁少康), Dengyu Zhu(朱登玉), Yuming Bai(白宇明), Tao Wang(王韬), Fufu Liu(刘福福), Lulu Pan(潘禄禄), Cunfang Feng(冯存芳), Bohan Zhang(张博涵), Daping He(何大平), and Shengxiang Wang(汪胜祥)

Citation: Chin. Phys. B, 2024, 33 (**3**): 037506. DOI: 10.1088/1674-1056/acfafa
Journal homepage: http://cpb.iphy.ac.cn; http://iopscience.iop.org/cpb

What follows is a list of articles you may be interested in

Effect of seed layers on the static and dynamic magnetic properties of CoIr films with negative effective magnetocrystalline anisotropy

Tianyong Ma(马天勇), Sha Zhang(张莎), Chenhu Zhang(张晨虎), Zhiwei Li(李志伟), Tao Wang(王涛), and Fashen Li(李发伸)

Chin. Phys. B, 2023, 32 (**12**): 127503. DOI: 10.1088/1674-1056/acd523

Low-temperature ferromagnetism in tensile-strained $LaCoO_{2.5}$ thin film

Yang-Yang Fan(范洋洋), Jing Wang(王晶), Feng-Xia Hu(胡凤霞), Bao-He Li(李宝河), Ai-Cong Geng(耿爱丛), Zhuo Yin(殷卓), Cheng Zhang(张丞), Hou-Bo Zhou(周厚博), Meng-Qin Wang(王梦琴), Zi-Bing Yu(尉紫冰), and Bao-Gen Shen(沈保根)

Chin. Phys. B, 2023, 32 (**8**): 087504. DOI: 10.1088/1674-1056/acafdc

Electric-field control of perpendicular magnetic anisotropy by resistive switching via electrochemical metallization

Yuan Yuan(袁源), Lu-Jun Wei(魏陆军), Yu Lu(卢羽), Ruo-Bai Liu(刘若柏), Tian-Yu Liu(刘天宇), Jia-Rui Chen(陈家瑞), Biao You(游彪), Wei Zhang(张维), Di Wu(吴镝), and Jun Du(杜军)

Chin. Phys. B, 2023, 32 (**6**): 067505. DOI: 10.1088/1674-1056/acbde8

Enhancement of spin-orbit torque efficiency by tailoring interfacial spin-orbit coupling in Pt-based magnetic multilayers

Wenqiang Wang(王文强), Gengkuan Zhu(朱耿宽), Kaiyuan Zhou(周恺元), Xiang Zhan(战翔), Zui Tao(陶醉), Qingwei Fu(付清为), Like Liang(梁力克), Zishuang Li(李子爽), Lina Chen(陈丽娜), Chunjie Yan(晏春杰), Haotian Li(李浩天), Tiejun Zhou(周铁军), and Ronghua Liu(刘荣华)

Chin. Phys. B, 2022, 31 (**9**): 097504. DOI: 10.1088/1674-1056/ac76aa

Voltage control magnetism and ferromagnetic resonance in an $Fe_{19}Ni_{81}$/PMN-PT heterostructure by strain

Jun Ren(任军), Junming Li(李军明), Sheng Zhang(张胜), Jun Li(李骏), Wenxia Su(苏文霞), Dunhui Wang(王敦辉), Qingqi Cao(曹庆琪), and Youwei Du(都有为)

Chin. Phys. B, 2022, 31 (**7**): 077502. DOI: 10.1088/1674-1056/ac43ab

---

Enhanced resonance frequency in Co_2FeAl thin film with different thicknesses grown on flexible graphene substrate

Cai Zhou(周偲)[1,3], Shaokang Yuan(袁少康)[2,3], Dengyu Zhu(朱登玉)[2,3], Yuming Bai(白宇明)[4], Tao Wang(王韬)[4], Fufu Liu(刘福福)[5], Lulu Pan(潘禄禄)[6], Cunfang Feng(冯存芳)[1,3], Bohan Zhang(张博涵)[1,3,†], Daping He(何大平)[7], and Shengxiang Wang(汪胜祥)[1,3,‡]

[1] *Hubei Engineering and Technology Research Center for Functional Fiber Fabrication and Testing, Wuhan Textile University, Wuhan* 430200, *China*
[2] *School of Electronic and Electrical Engineering, Wuhan Textile University, Wuhan* 430200, *China*
[3] *School of Mathematical and Physical Sciences, Wuhan Textile University, Wuhan* 430200, *China*
[4] *School of Integrated Circuits, Huazhong University of Science and Technology, Wuhan* 430074, *China*
[5] *Key Laboratory for Magnetism and Magnetic Materials, Ministry of Education, Lanzhou University, Lanzhou* 730000, *China*
[6] *Beijing National Center for Condensed Matter Physics and Institute of Physics, Chinese Academy of Sciences, Beijing* 100190, *China*
[7] *Hubei Engineering Research Center of RF-Microwave Technology and Application, Wuhan University of Technology, Wuhan* 430070, *China*

(Received 8 August 2023; revised manuscript received 18 September 2023; accepted manuscript online 19 September 2023)

The flexible materials exhibit more favorable properties than most rigid substrates in flexibility, weight saving, mechanical reliability, and excellent environmental toughness. Particularly, flexible graphene film with unique mechanical properties was extensively explored in high frequency devices. Herein, we report the characteristics of structure and magnetic properties at high frequency of Co_2FeAl thin film with different thicknesses grown on flexible graphene substrate at room temperature. The exciting finding for the columnar structure of Co_2FeAl thin film lays the foundation for excellent high frequency property of Co_2FeAl/flexible graphene structure. In-plane magnetic anisotropy field varying with increasing thickness of Co_2FeAl thin film can be obtained by measurement of ferromagnetic resonance, which can be ascribed to the enhancement of crystallinity and the increase of grain size. Meanwhile, the resonance frequency which can be achieved by the measurement of vector network analyzer with the microstrip method increases with increasing thickness of Co_2FeAl thin film. Moreover, in our case with graphene film, the resonance magnetic field is quite stable though folded for twenty cycles, which demonstrates that good flexibility of graphene film and the stability of high frequency magnetic property of Co_2FeAl thin film grown on flexible graphene substrate. These results are promising for the design of microwave devices and wireless communication equipment.

Keywords: enhanced resonance frequency, magnetic resonance field, flexible graphene substrate

PACS: 75.70.–I, 76.50.+g, 32.30.Dx **DOI:** 10.1088/1674-1056/acfafa

1. Introduction

Recently, with improvement in the standard of living, the flexible electronic devices have received wide attention owing to perfect stretchability, low cost, biocompatibility, and light weight, which have great potential in application of sensitive skin, flexible circuit boards, and paper-like displays. In these flexible materials, the advanced carbon material-based films, including carbon fibers,[1] carbon nanotubes,[2–4] multi-shelled fullerenes,[5,6] and especially graphene,[7,8] exhibit more favorable properties than most rigid substrates in flexibility, weight saving, mechanical reliability, and excellent environmental toughness. The flexible graphene films can be extensively explored in high frequency devices due to the unique mechanical properties.[9–11] He's group has reported flexible graphene films for radio-frequency antennas, multi-beam radiation, highly sensitive wearable sensor, etc.[12–14] In fact, the graphene film as flexible substrate is expected to Heusler metallic materials are considered to be ideal compounds as high spin polarized current sources, and some of them generally have a high Curie temperature, high spin polarization and low damping,[15,16] Among the Heusler metallic materials, with the formula of X_2YZ (where X is a transition metal element, Y is another transition metal element, and Z is a main group sp element), particularly Co_2FeAl (CFA), have attracted intense research interest due to the half-metals even at room temperature.[17–19] Belmeguenai's research group have investigated the static and dynamic magnetic property in CFA thin films by sputtering on Si and MgO substrates annealed at different temperatures.[20] Our group has reported the electric field tuning magnetic anisotropy in CFA thin film grown on PMN-PT substrate.[21,22] In these cases, the CFA thin film was fabricated on the above conventional rigid substrate. This greatly limits the application scope of flexible thin film materials. Therefore, it is essential to study the magnetic properties of magnetic thin films fabricated on flexible substrate. In this work, the high frequency property of CFA thin film with different thicknesses grown on flexible graphene substrate (FGS) is analyzed in detail at room temperature. With the thickness of

†Corresponding author. E-mail: bhzhang@wtu.edu.cn
‡Corresponding author. E-mail: shxwang@wtu.edu.cn

© 2024 Chinese Physical Society and IOP Publishing Ltd

CFA thin film grown on FGS varying from 20 nm to 200 nm, the increase of grain size can be obtained. The in-plane magnetic anisotropy field decreases with increasing the thickness of CFA thin film from 20 nm to 100 nm measured by ferromagnetic resonance, which can be attributed to the change of structure of CFA thin film with different thicknesses grown on FGS. However, in-plane magnetic anisotropy field increases with continuing to increase thickness to 200 nm, which can lead to the resonance frequency shifting to higher frequency measured by using a vector network analyzer with the microstrip method.

2. Experimental details

The CFA thin films with different thicknesses (20 nm, 50 nm, 100 nm, 150 nm, and 200 nm) were deposited by direct current (DC) magnetron sputtering on FGS at a common base pressure $< 8 \times 10^{-4}$ Pa and work processing Ar pressure of 0.1 Pa, a power of 150 W. A field emission scanning electron microscope (SEM, Hitachi SU5000) was employed to observe the cross-section microstructures and the surface morphologies. The x-ray diffraction (XRD) measurements were performed on X'Pert x-ray powder diffractometer with Cu K_α radiation (1.54056 Å). The ferromagnetic resonance (FMR) measurements were carried out with a PNA 8722ES vector network analyzer using the coplanar waveguide method. Permeability spectra were carried out with a PNA E8363B vector network analyzer using the microstrip method.

3. Results and discussion

The cross-sectional and highly magnified SEM images of the FGS show that the film based on orderly stacked graphene layers with a thickness of 108 μm as shown in Figs. 1(b) and 1(c). The cross-section image of CFA thin film with different thicknesses grown on FGS is also observed by SEM. For brevity, only the 200 nm-thick CFA grown on FGS is shown in Fig. 1(a). The columnar structure of CFA can be obviously observed, which is comparable to the sample grown on Si substrate.[23,24] The exciting finding lays the foundation for the good quality of CFA/FGS structure. In addition, surface morphologies of the CFA/FGS structure with various thicknesses are shown in the inset of Fig. 2(b). Firstly, the smooth surface morphologies of FGS can be obtained as shown in the top inset of Fig. 2(b). Then, we can observe that with increasing thickness of CFA thin film, the grain continues growth and corresponding size becomes larger. This result indicates thickness has a great influence on microstructure of CFA thin film grown on FGS.

A piece of rolled FGS is shown in the inset of Fig. 2(a), which demonstrates FGS has good flexibility. The crystal structures for all thin films were measured by XRD as shown

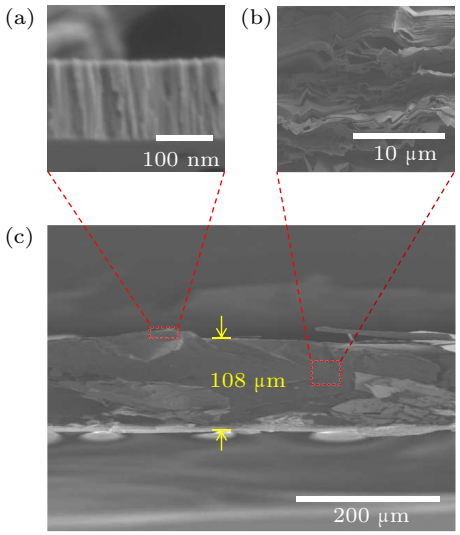


Fig. 1. The SEM cross-section images of (a) CFA thin film, (b) FGS and (c) CFA/FGS structure, respectively.

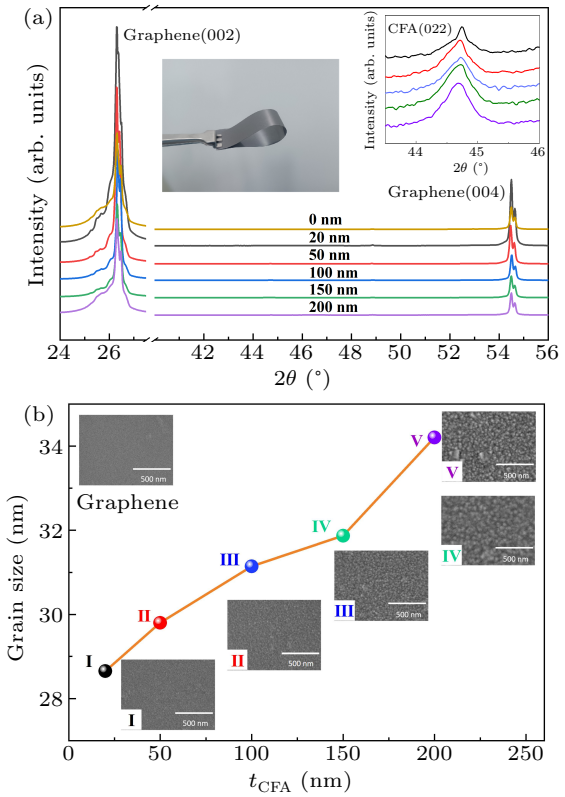


Fig. 2. (a) XRD patterns of CFA/FGS structure with different thicknesses of CFA thin film and (0 nm) pure graphene substrate. The inset shows digital photograph of FGS. (b) The grain size versus thickness of CFA thin film. The inset images show surface morphologies of CFA/FGS structure with different thicknesses and FGS.

in Fig. 2(a). The sharp diffraction peak (002) and peak (004) of FGS are located at 26.3° and 54.5°. The (022) peak of CFA thin film appears at 44.7°. Moreover, the intensity of (022) peak of CFA thin film increases with increasing thickness of CFA thin film as shown in the top inset of Fig. 2(a), which indicates the enhancement of crystallization. However, the position of (022) peak of CFA thin film remains unchanged. According to the Scherrer equation, grain sizes of CFA thin films

are 28.6 nm, 29.7 nm, 31.1 nm, 31.8 nm and 34.2 nm with increasing thickness of CFA thin films, respectively, as shown in Fig. 2(b), which is consistent with variation tendency of surface morphologies measured by SEM as shown in the inset of Fig. 2(b). The increase of grain size with increasing thickness of CFA thin film can indirectly influence the change of in-plane magnetic anisotropy field. The above results confirm the good quality of CFA/FGS structure we prepared, which has huge impact on the physical properties, especially high-frequency magnetic properties.

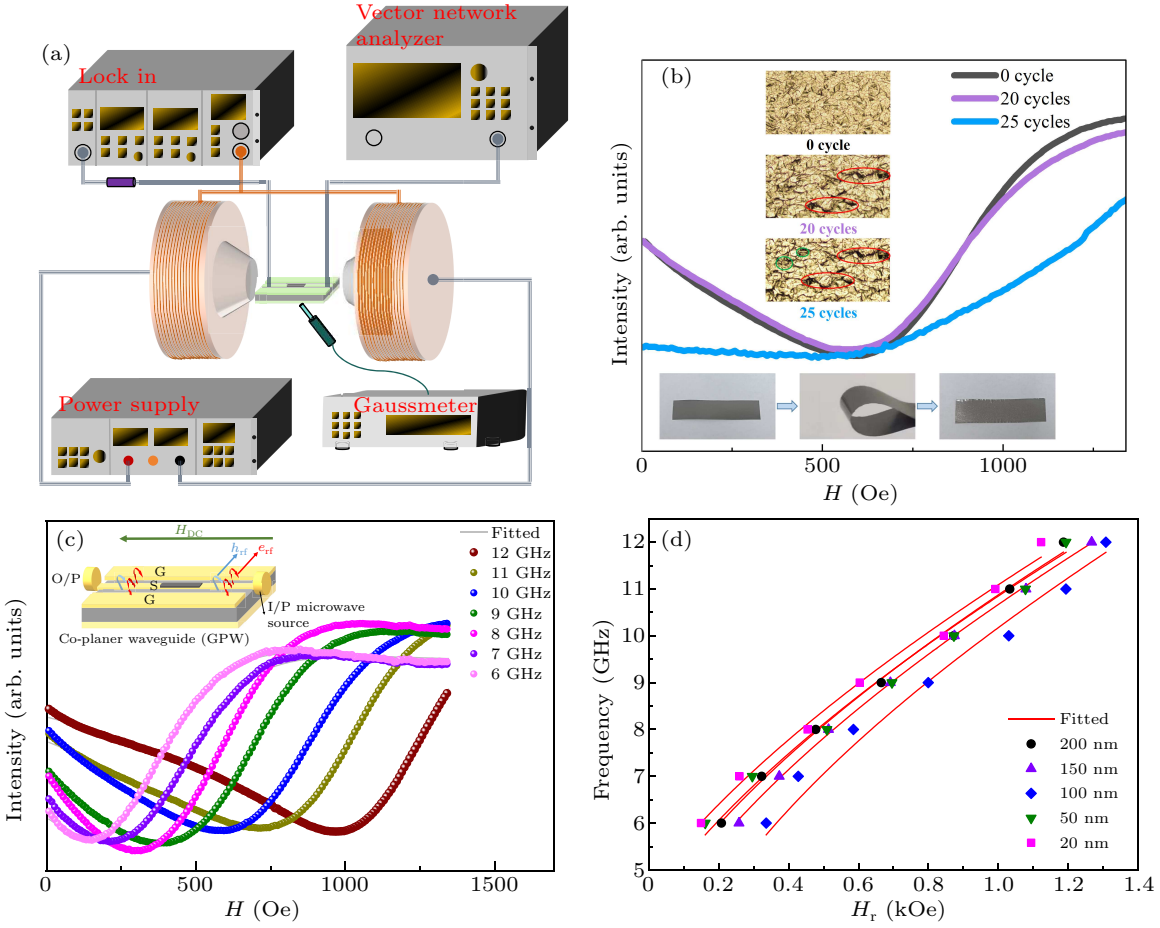


Fig. 3. (a) The schematic illustration of ferromagnetic resonance (FMR) using a vector network analyzer. (b) These curves under unfolded state, and after being fold twenty cycles and twenty-fifth cycles. The top inset shows more cracks with increasing folding cycles. The bottom inset shows the folding schematic diagram. (c) The experimental data (dots) and fitting curves (lines) of FMR for 150 nm-thick CFA thin film. The inset shows the device schematic of microstrip method. (d) The applied microwave frequency versus resonance magnetic field with different thicknesses of CFA thin film.

The high-frequency magnetic properties of CFA thin films were measured by ferromagnetic resonance (FMR) using a vector network analyzer with coplanar waveguide method as shown in Fig. 3(a) and the top inset of Fig. 3(c). In order to prove the good flexibility of graphene film and the stability of high frequency magnetic property of Co_2FeAl thin film grown on flexible graphene substrate, we choose the sample with 150-nm thick CFA thin film to fold over twenty cycles and then take FMR measurement at fixed 10 GHz every five cycles. The folding schematic diagram is shown in the bottom inset of Fig. 3(b). As shown in Fig. 3(b), the curves basically remain unchanged within twenty cycles. The resonance magnetic field of approximately 875 Oe is obtained by fitting these curves according to Eq. (1). However, the dramatic change of the FMR curve occurs in folding twenty-fifth cycles. The shape of curve becomes slightly shaking and the curve deforms, which indicates the quality of CFA thin film deteriorates after being folded twenty cycles. The more cracks can be distinctly observed after twenty cycles as shown in the top inset of Fig. 3(b), which can be measured by RX50M series metallurgical microscope. The similar result can be obtained for CFA thin film with 20 nm, 50 nm, 100 nm and 200 nm. Figure 3(c) shows under different frequencies the typical FMR spectra for 150 nm-thick CFA thin film. In general, the magnetization is probed using a special phase correlation under the microwave excitation, and the FMR spectrum does not correspond to the imaginary part of the susceptibility alone, but in fact represents a mixture of the imaginary and real parts. Therefore, the actual function of the absorption curve can be fitted by an asymmetric Lorentzian function[25]

$$\varphi(H) = A\frac{\Delta H\cos\delta + (H - H_{\rm r})\sin\delta}{\Delta H^2 + (H - H_{\rm r})^2}, \tag{1}$$

where H is the external magnetic field, H_r is the magnetic resonance field, ΔH is the half-width at half-maximum of the linewidth, δ is the phase that mixes the real and imaginary parts of the dynamic susceptibility, and A is the integral coefficient. The fitting solid curve is shown in Fig. 3(c) in light gray color. The fitting result reveals that H_r shifts towards higher magnetic field with increasing frequency. For 150 nm-thick CFA thin film, the resonance magnetic field increases from 0.258 kOe to 1.268 kOe with the microwave frequency increasing from 6 GHz to 12 GHz as shown in Fig. 3(c). In addition, frequency-dependent $\varphi(H)$ curves were measured for all thin films. As a result, the data of frequency-dependent H_r under different thicknesses of CFA thin film are shown in Fig. 3(d), which is fitted using the Kittel's equation[26]

$$f = \frac{\gamma}{2\pi}\sqrt{(H_r + H_k)(H_r + H_k + 4\pi M_s)}, \tag{2}$$

where gyromagnetic ratio $\gamma/2\pi = 2.8$ GHz/kOe,[27,28] $4\pi M_s$ is the saturation magnetization, and H_k is the in-plane magnetic uniaxial anisotropy field. The data of frequency-dependent H_r was fitted using Eq. (2) to extract $4\pi M_s$ and H_k. The fitting curve is shown in Fig. 3(d) with red color. With increasing thickness of CFA thin film, the value of $4\pi M_s$ is almost unchanged. However, H_k is found to decrease from 0.243 kOe to 0.062 kOe with increasing thickness from 20 nm to 100 nm as shown in Fig. 4(a). This can be explained as follows. The crystallization of CFA thin film is enhanced with the increase of thickness of CFA thin film as shown in the inset of Fig. 2(b). Meanwhile, the grain size becomes larger. The competition between uniaxial magnetic anisotropy and magnetocrystalline anisotropy can appear, which can lead to the decrease of in-plane magnetic uniaxial anisotropy field. Nevertheless, H_k increases from 0.134 kOe to 0.180 kOe with thicknesses increasing from 150 nm to 200 nm. The sudden increase in H_k for CFA thin film with 150 nm-thick can be attributed to releasing of substrate induced strain,[29] which can lead to the higher resonance frequency.

The dependence of permeability on the frequency with different thicknesses of CFA thin film was measured using a vector network analyzer with the microstrip method, as shown in the bottom inset of Fig. 4(b). When the thickness of CFA thin film is less than 100 nm, there is no resonance peak detected in this method, which can be attributed to the disorderly arrangement of magnetic moment. This is related to roughness of surface morphologies. With continuing to increase the thickness of CFA thin film, the resonance peak can be obviously observed for CFA thin film with 150 nm and 200 nm-thick. The resonance frequency enhances from 3.4 GHz to 5.6 GHz, which is consistent with the result of H_k-dependent thickness of CFA thin film. Moreover, the resonance magnetic field and resonance frequency are quite stable though folded over ten times, which demonstrates that good flexibility of graphene film and the ultrastability of high frequency property of CFA thin film grown on FGS.

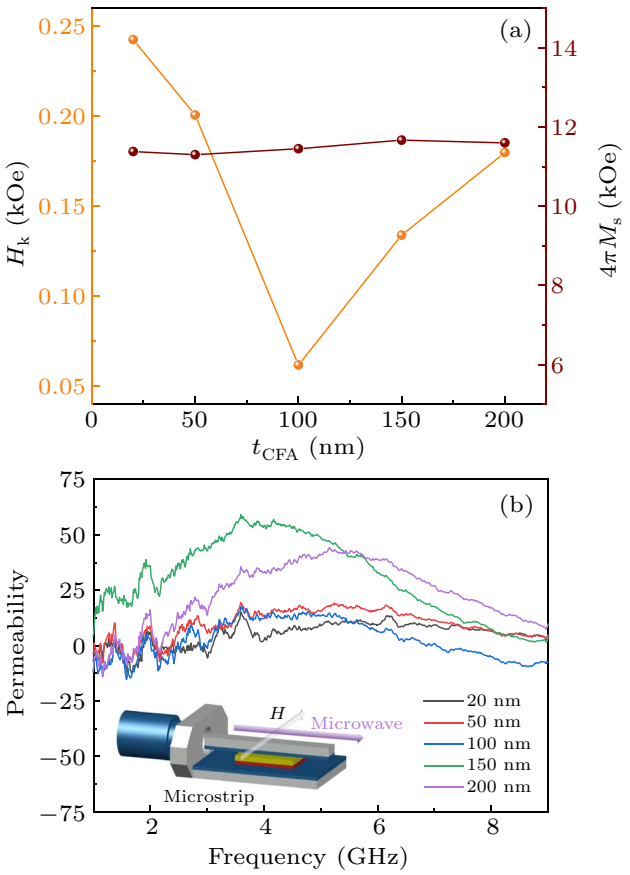


Fig. 4. (a) The change of H_k and $4\pi M_s$ with different thicknesses of CFA thin film. (b) The permeability spectra of CFA thin film. The inset shows the device schematic of coplanar waveguide method.

4. Conclusion

In summary, we identified characteristics of CFA/FGS structure and high frequency magnetic property of CFA thin film with different thicknesses grown on FGS. With increasing thickness of CFA thin film, the surface becomes smoother, and grain size gradually increases, which can influence the change of in-plane magnetic anisotropy field. The in-plane magnetic anisotropy field gradually decreases when the thickness of CFA thin film increases from 20 nm to 100 nm by measurement of FMR. However, with thickness increasing to 100 nm, in-plane magnetic anisotropy field suddenly increases. The measurement result of the dependence of permeability on the frequency demonstrates that the resonance peak can be obviously observed at 3.4 GHz and 5.6 GHz with thickness 150 nm and 200 nm, which is in agreement with the result of FMR. Moreover, the high frequency parameter remains stable though folded over twenty cycles, which indicates the good flexibility of graphene film and the ultrastability of high frequency property of CFA thin film grown on FGS. These results can be used to remove the obstacles that communication system transmission distance and signal quality.

Acknowledgments

Project supported by the National Natural Science Foundation of China (Grant Nos. 51901163 and 12104171) and the Fundamental Research Funds for the Central Universities (Grant No. 2021XXJS025).

References

[1] Mehdlpour A, Trueman C W, Sebak A R and Hoa S V 2009 *IEEE Antennas and Propagation Society International Symposium*, North Charleston, SC, USA, 2009, pp. 1–4
[2] Rutherglen C, Jain D and Burke P 2009 *Nat. Nanotechnol.* **4** 811
[3] Elwi T A, Al-Rizzo H M, Rucker D G, Dervishi E, Li Z and Biris A S 2010 *Nanotechnology* **21** 045301
[4] Puchades I, Rossi J E, Cress C D, Naglich E and Landi B J 2016 *ACS Appl. Mater. Interfaces.* **8** 20986
[5] Vacirca N A, McDonough J K, Jost K, Gogotsi Y and Kurzweg T P 2013 *Appl. Phys. Lett.* **103** 073301
[6] Shenderova O, Grishko V, Cunningham G, Moseenkov S, McGuire G and Kuznetsov V 2008 *Diam. Relat. Mater.* **17** 462
[7] Sajal S Z, Braaten B D and Marinov V R 2015 *IEEE International Symposium on Antennas and Propagation & USNC/URSI National Radio Science Meeting*, Vancouver, BC, Canada, 2015, pp. 2415–2416
[8] Sa'don S N H, Kamarudin M R, Ahmad F, Jusoh M and Majid H A 2017 *Appl. Phys. A* **123** 118
[9] Takeichi T, Eguchi Y, Kaburagi Y, Hishiyama Y and Inagaki M 1999 *Carbon* **37** 569
[10] Ubbelohde A R 1976 *Carbon* **14** 1
[11] Hishiyama Y, Nakamura M, Nagata Y and Inagaki M 1994 *Carbon* **32** 645
[12] Fan C, Wu B, Song R G, Zhao Y T, Zhang Y H and He D P 2019 *Carbon* **155** 506
[13] Song R G, Mao B Y, Wang Z, Hui Y Y, Zhang N, Fang R, Zhang J W, Wu Y, Ge Q, Novoselov K S and He D P 2023 *Proc. Natl. Acad. Sci. USA* **120** e2209807120
[14] Qian W, Fu H Q, Sun Y, Wang Z, Wu H, Kou Z K, Li B W, He D P and Nan C W 2022 *Adv. Mater.* **34** 2206101
[15] de Groot R A, Mueller F M, van Engen P G and Buschow K H J 1983 *Phys. Rev. Lett.* **50** 2024
[16] Felser C and Hillebrands B 2007 *J. Phys. D: Appl. Phys.* **40** E01
[17] Gabor M S, Petrisor T, Tiusan C, Hehn M and Petrisor T 2011 *Phys. Rev. B* **84** 134413
[18] Cui Y S, Khodadadi B, Schäfer S, Mewes T, Lu J W and Wolf S A 2013 *Appl. Phys. Lett.* **102** 162403
[19] Gupta R, Husain S, Kumar A, Brucas R, Rydberg A and Svedlindh P 2021 *Adv. Opt. Mater.* **9** 2001987
[20] Belmeguenai M, Tuzcuoglu H, Gabor M S, Petrisor Jr T, , Tiusan C, Zighem F, Chérif S M and Moch P 2014 *J. Appl. Phys.* **115** 043918
[21] Zhou C, Dunzhu G S, Yao J L and Jiang C J 2017 *J. Alloys Compd.* **710** 680
[22] Zhou C, Wang F L, Dunzhu G S, Yao J L and Jiang C J 2016 *J. Phys. D: Appl. Phys.* **49** 455001
[23] Wang G X, Dong C H, Wang W X, Wang Z L, Chai G Z, Jiang C J and Xue D S 2012 *J. Appl. Phys.* **112** 093907
[24] Zhou C, Wang F L, Wei W W, Wang G X, Jiang C J and Xue D S 2013 *J. Phys. D: Appl. Phys.* **46** 425002
[25] Mecking N, Gui Y S and Hu C M 2007 *Phys. Rev. B* **76** 224430
[26] Kittel C 1948 *Phys. Rev. B* **73** 155
[27] Song N N, Gu S Z, Wu Q, Li C L, Zhou J, Zhang P P, Wang W and Yue M 2018 *J. Magn. Magn. Mater.* **451** 793
[28] Holanda J, Saglam H, Karakas V, Zang Z Z, Li Y, Divan R, Liu Y Z, Ozatay O, Novosad V, Pearson J E and Hoffmann A 2020 *Phys. Rev. Lett.* **124** 087204
[29] Kipgen L, Fulara H, Raju M and Chaudhary S 2012 *J. Magn. Magn. Mater.* **324** 3118